Mon. Not. R. Astron. Soc. **392,** L35–L39 (2009) doi:10.1111/j.1745-3933.2008.00579.x

The history of star formation and mass assembly in early-type galaxies

M. S. Clemens,[1] A. Bressan,[1,2,3]★ B. Nikolic[4] and R. Rampazzo[1]

[1]*INAF–Osservatorio Astronomico di Padova, Vicolo dell'Osservatorio, 5, 35122 Padova, Italy*
[2]*SISSA–ISAS, International School for Advanced Studies, via Beirut 4, 34014 Trieste, Italy*
[3]*INAOE, Luis Enrique Erro 1, 72840, Tonantzintla, Puebla, Mexico*
[4]*Astrophysics Group, Cavendish Laboratory, Madingley Road, Cambridge CB3 0HE*

Accepted 2008 October 21. Received 2008 October 21; in original form 2008 September 6

ABSTRACT

We define a volume-limited sample of over 14 000 early-type galaxies (ETGs) selected from Data Release 6 of the Sloan Digital Sky Survey. The density of environment of each galaxy is robustly measured. By comparing narrow-band spectral line indices with recent models of simple stellar populations (SSPs), we investigate trends in the star formation history as a function of galaxy mass (velocity dispersion), density of environment and galactic radius. We find that age, metallicity and α-enhancement all increase with galaxy mass and that field ETGs are younger than their cluster counterparts by $\sim$2 Gyr. We find negative radial metallicity gradients for all masses and environments, and positive radial age gradients for ETGs with velocity dispersion over 180 km s^{-1}. Our results are qualitatively consistent with a relatively simple picture for ETG evolution in which the low-mass haloes accreted by a protoETG contained not only gas but also a stellar population. This fossil population is preferentially found at large radii in massive ETGs because the stellar accretions were dissipationless. We estimate that the typical, massive ETG should have been assembled at $z \lesssim 3.5$. The process is similar in the cluster and field but occurred earlier in dense environments.

Key words: galaxies: abundances – galaxies: elliptical and lenticular, cD – galaxies: formation.

1 INTRODUCTION

Observational determinations of the history of star formation in early-type Galaxies (ETGs) are of great importance because hierarchical models of galaxy formation make firm predictions for the relation between age, metallicity and α-enhancement as a function of mass. These scaling relations, plotted against the observational proxy for mass, the velocity dispersion (hereafter σ), have been the focus of many recent studies of ETGs (Kuntschner et al. 2002; Terlevich & Forbes 2002; Proctor et al. 2004; Nelan et al. 2005, hereafter N05; Thomas et al. 2005; Bernardi et al. 2006; Gallazzi et al. 2006; Sánchez-Blázquez et al. 2006; Annibali et al. 2007; de la Rosa et al. 2007; Jimenez et al. 2007; Kuntschner et al. 2001; Lucey et al. 2007; Mateus et al. 2007; Smith, Lucey & Hudson 2007; Proctor et al. 2008).

These studies clearly show that the simple picture of early formation of low-mass galaxies, which then merge to form more massive systems, is incorrect. The oldest stellar populations are found in the most massive galaxies – one aspect of so-called 'downsizing'. However, the observational constraint is sensitive to the epoch at which star formation ceased, not when it started, so that low-mass ETGs can still be 'old', as dynamically bound objects, but have a *mean* stellar age that is much younger. However, this is not sufficient to save the simple hierarchical picture because the α-enhancement is also seen to increase with mass – implying more rapid formation for massive objects. This is a prediction of monolithic collapse models. It is important to remember that both the star formation history and mass assembly history of ETGs determine their evolution.

The most common method of determining the age, metallicity and α-enhancement of ETGs is by comparison of the narrow-band absorption-line indices with simple stellar population (SSP) models. It is well known that stellar population parameters based on these indices are also sensitive to minor episodes of recent star formation. Luminosity-weighted, SSP equivalent stellar population parameters, such as those discussed here, do not, therefore, distinguish between a genuinely young galaxy and an old galaxy that has experienced a 'rejuvenation' event (sometimes called 'frosting').

Some recent studies based on the colour–magnitude relation of ETGs using colours that are extremely sensitive to recent star formation, in fact paint a surprising picture of ETG evolution. Schawinski et al. (2007) have used Galaxy Evolution Explorer (GALEX) ultraviolet imaging to show that 30 per cent of massive ETGs show *ongoing* star formation and that this fraction is higher in low-density environments. A similar picture is given by mid-infrared *Spitzer* data. Both Clemens et al. (2008) and Bressan et al. (2006) find that $\sim$30 per cent of ETGs in the Coma and Virgo clusters have experienced some star formation in the recent past.

★E-mail: marcel.clemens@oapd.inaf.it

A recent study by Rogers et al. (2007) has combined Sloan Digital Sky Survey (SDSS) spectra and GALEX data to conclude that 'weak episodes of recent star formation' are a phenomenon more commonly associated with ETGs in the *cluster* environment, a result seemingly, but not necessarily, inconsistent with several studies that find older SSP equivalent ages in denser environments.

Here, we repeat the analysis carried out in Clemens et al. (2006, hereafter Paper I), which used 3614 objects selected from Data Release 3 (DR3) of the SDSS. Applying the same selection criteria to DR6, we define a sample of 14 353 ETGs, four times as many objects.

2 SAMPLE SELECTION AND DATA ANALYSIS

Sample selection is identical to that described in Paper I. The local environmental density is defined as the inverse of the distance to the fifth-nearest neighbour, $1/r_5$, corrected for the redshift-dependent effect of survey boundaries. The sample is limited to the redshift range, $0.01 < z < 0.1$.

We measure the 21 line-strength indices of the original Lick-IDS system plus the additional indices HγF, HδF, B4000 and HK. However, before measuring the narrow-band indices from each of the SDSS, spectra we smooth the spectra to the wavelength-dependent resolution of the Lick-IDS. This step is essential as the models that we use to derive the age, metallicity and α-enhancement are based on the Lick system. The index values are then corrected for the smoothing effects of the galaxy's velocity dispersion and aperture corrected to a standard normalized radius (a fraction of the half-light radius). See Paper I for a more detailed description.

Besides being based on DR6, this work differs from that of Paper I only in two respects. First, in Paper I, we chose to correct for the fixed angular diameter of 3 arcsec sampled by the SDSS fibre using the radial index measurements of 50 nearby E and S0 galaxies (Rampazzo et al. 2005). Here, we make use of the *r*-band effective radii provided in the SDSS catalogue to derive the aperture correction directly. Statistically, a more reliable correction should be obtained in this way. However, this also means that we must choose a larger standard radius to which to correct ($r_e/10$ was used in Paper I). Typically, the 3 arcsec diameter SDSS fibre samples $\sim r_e/2$, with very few objects being so large that the fibre samples $r_e/10$. To avoid extrapolating beyond measured radii, we therefore aperture correct to a standard radius of either $r_e/2$ or $r_e/4$.

A plot of index value versus the fraction of r_e sampled by the fibre will show a gradient. However, the gradient is due not only to the radial gradients within each galaxy but also to the correlation between r_e and σ. Because index values are correlated with σ, this effect increases the magnitude of the gradient. To determine the aperture effect, we therefore consider the variation of index value as a function of the fraction of r_e sampled by the fibre in restricted bins of σ. In this way, we minimize the effect of the index–σ relations and determine the radial index gradients as a function of σ. We plot index values as a function of r/r_e in five bins, for eight separate bins of σ. The bins are chosen to maintain a large number of objects in each bin and gradients are then derived by weighting each point by $\sqrt{n}$, where n is the number in the bin. The values of the radial index gradients and their variation with σ are shown in Table 1.

We use the radial index gradients to correct our index values for aperture effects. First, we use the measured value of σ for a given galaxy to determine the value of the radial index gradient ΔI:

$$\Delta I = (\sigma_{200} - 1)\,\frac{\mathrm{d}\Delta I}{\mathrm{d}\sigma_{200}} + \Delta I_{200}, \qquad (1)$$

Table 1. Radial index gradients as a function of velocity dispersion, σ. The radial index gradients are expressed as $\Delta I = \frac{\mathrm{d}I}{\mathrm{d}\log(r/r_e)}$, where I is the value of the index. The third column gives values for the dependence of the radial index gradients on σ in units of 200 km s^{-1}, σ_{200} . ΔI_{200} is the value of the index gradient at $\sigma = 200\,\mathrm{km\,s^{-1}}$. These parameters have been used in the aperture correction of all indices. Most indices show a well-defined radial gradient, but rather few show a convincing trend of this gradient on σ. The last column shows the ratio of the gradient in the third column and its error and so is an estimate of the statistical significance of the gradient as a function of σ. For those indices whose radial gradients show little trend with σ, the value of ΔI_{200} is a good measure of the radial gradient for galaxies of any σ.

Index	ΔI_{200}	$\mathrm{d}\Delta I/\mathrm{d}\sigma_{200}$	S/N
CN1 (mag)	-0.019 ± 0.002	-0.005 ± 0.008	0.6
CN2 (mag)	-0.018 ± 0.002	-0.010 ± 0.009	1.1
Ca4227	-0.113 ± 0.014	0.060 ± 0.065	0.9
G4300	-0.012 ± 0.031	0.379 ± 0.149	2.5
Fe4383	-0.423 ± 0.040	0.600 ± 0.188	3.2
Ca4455	-0.121 ± 0.017	-0.008 ± 0.081	0.1
Fe4531	-0.188 ± 0.030	0.203 ± 0.142	1.4
C4668	-1.039 ± 0.057	-0.561 ± 0.282	2.0
Hβ	0.085 ± 0.021	-0.488 ± 0.105	4.7
Fe5015	-0.415 ± 0.043	-0.401 ± 0.201	2.0
Mg1 (mag)	-0.024 ± 0.001	0.013 ± 0.005	2.5
Mg2 (mag)	-0.028 ± 0.001	0.013 ± 0.007	2.0
Mgb	-0.311 ± 0.028	0.286 ± 0.128	2.2
Fe5270	-0.173 ± 0.023	0.066 ± 0.112	0.6
Fe5335	-0.241 ± 0.026	-0.134 ± 0.127	1.1
Fe5406	-0.150 ± 0.022	0.010 ± 0.108	0.1
Fe5709	-0.053 ± 0.015	-0.052 ± 0.074	0.7
Fe5782	-0.103 ± 0.015	0.058 ± 0.071	0.8
NaD	-0.627 ± 0.037	-0.546 ± 0.173	3.1
TiO1 (mag)	-0.000 ± 0.001	0.004 ± 0.002	1.9
TiO2 (mag)	-0.008 ± 0.001	0.002 ± 0.002	0.8
B4000	0.017 ± 0.002	-0.013 ± 0.007	1.9
HK	0.001 ± 0.002	-0.028 ± 0.012	2.4
HδF	0.265 ± 0.030	-0.265 ± 0.144	1.8
HγF	0.290 ± 0.031	-0.558 ± 0.154	3.6

where σ_{200} is the velocity dispersion in units of 200 km s^{-1} and ΔI_{200} is the value of the index gradient for $\sigma = 200\,\mathrm{km\,s^{-1}}$. The values for $\mathrm{d}\Delta I/\mathrm{d}\sigma_{200}$ and ΔI_{200} are given in Table 1.

This value of the radial index gradient is then used with the measured value of r_e of the galaxy to correct the index value to the equivalent radius, $r = r_e/2$ or $r_e/4$:

$$I_c = I + \Delta I\ \log(r r_e/1''.5), \qquad (2)$$

where I_c is the corrected index, I is the measured index value, r_e is the effective radius of the galaxy in arcsec and r is the standard radius expressed as a fraction of r_e (0.5 or 0.25 here).

The use of the effective radii provided in SDSS (the Petrosian half-light radius) to affect the aperture correction has one caveat; i.e. these radii are not seeing corrected. Therefore, for galaxies with a small angular diameter, r_e is overestimated. Median *r* band seeing for SDSS imaging is 1.4 arcsec (Adelman-McCarthy et al. 2007, fig. 4) and the median effective diameter for our sample is 5 arcsec. We believe, however, that this is not a serious problem because the seeing also alters the light entering the spectroscopic fibre. The considerable agreement we find in values for the indices as a function of σ with other studies (see below) supports this view.

The second difference from Paper 1 is the removal of one index, G4300, from the fitting procedure used to derive the age, metallicity

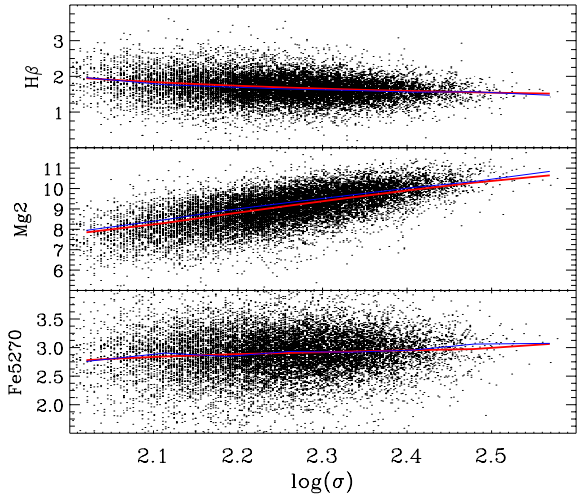

Figure 1. A posteriori comparison of the models with selected indices (only three are shown but all indices are similarly reproduced). The thick red lines are the simultaneous solution to the whole set of indices (not fits for each index), while the blue lines trace the median data value.

and α-enhancement. We found that the inclusion of the G4300 index worsened the post-priori model fit (Fig. 1) for all indices. Since no other index has this effect, this implies that this specific index is not well modelled (Annibali et al. 2007).

3 RESULTS

Here, we will use the index values to derive various evolutionary parameters as a function of σ, environment and galaxy radius. Before that, however, we briefly evaluate various trends seen in the fully σ and aperture-corrected index values.

3.1 Index values as a function of velocity dispersion

In Table 2, we show the corrected index values as a function of σ. Because the values refer to indices aperture corrected to $r_e/2$, they are not directly comparable to those of Paper I, where corrections were made to $r_e/10$. None the less, most indices show similar behaviour to those of Paper I. We briefly note here some of the larger differences seen in important indices (we refer to gradients expressed as $\mathrm{d}I/\mathrm{dlog}(\sigma)$ as a_1 and those as $\mathrm{dlog}\,I/\mathrm{dlog}(\sigma)$ as A_1).

C4668. The gradient of $a_1 = +4.4$ much larger than that of Paper I ($+1.8$). This value is closer to the value of $+5.2$ found by N05.

Hβ. The gradient of -1.0 ($A_1 = -0.24$) is shallower (-1.7 in Paper I). This value is in excellent agreement with Bernardi et al. (2003, hereafter B03) ($A_1 = -0.24$) and N05 ($a_1 = -1.2$).

Fe5015. The gradient of $a_1 = -1.5$ in Paper I contrasts to the present value of $+1.6$. This is much more consistent with N05 who find $a_1 = +1.0$.

Mg2. The value of $a_1 = 0.22$ is similar to that of Paper I, but is now more consistent with both B03 and Kuntschner et al. (2002).

Mgb. The gradient of $a_1 = 3.3$ ($A_1 = 0.37$) compares with 3.7 in Paper I. This is closer to that of B03 ($A_1 = 0.32$) and N05 ($a_1 = 3.2$).

Fe5270. In Paper I, a null gradient was found. The present value of $a_1 = +0.62$ is consistent with N05 who find an identical value.

We note, that globally, the new index gradients are much closer to those derived by N05 despite the fact that these authors aperture-corrected index values to a fixed physical radius, rather than to a fixed fraction of r_e as done here.

Table 2. Index values as a function of velocity dispersion, σ. The indices have been aperture corrected to a standard radius of $r_e/2$. Straight line fit parameters are given as the gradient, $a_1 = \mathrm{d}I/\mathrm{dlog}(\sigma)$, and intercept, a_0, of plots of index versus $\log\sigma$.

Index	$a_1 = \mathrm{d}\,I/\mathrm{d}\log(\sigma)$	a_0
CN1 (mag)	0.209 ± 0.002	-0.413 ± 0.005
CN2 (mag)	0.224 ± 0.003	-0.416 ± 0.006
Ca4227	0.400 ± 0.020	0.190 ± 0.046
G4300	1.118 ± 0.047	2.758 ± 0.106
Fe4383	1.759 ± 0.061	0.699 ± 0.136
Ca4455	0.628 ± 0.024	-0.172 ± 0.053
Fe4531	1.184 ± 0.044	0.544 ± 0.100
C4668	4.392 ± 0.083	-3.516 ± 0.187
Hβ	-1.033 ± 0.032	4.032 ± 0.073
Fe5015	1.604 ± 0.061	1.242 ± 0.137
Mg1 (mag)	0.145 ± 0.002	-0.217 ± 0.004
Mg2 (mag)	0.216 ± 0.002	-0.236 ± 0.005
Mgb	3.305 ± 0.057	-3.325 ± 0.128
Fe5270	0.617 ± 0.038	1.427 ± 0.085
Fe5335	0.922 ± 0.039	0.495 ± 0.087
Fe5406	0.563 ± 0.032	0.384 ± 0.072
Fe5709	-0.148 ± 0.021	1.206 ± 0.047
Fe5782	0.348 ± 0.026	-0.015 ± 0.059
NaD	4.432 ± 0.049	-6.345 ± 0.110
TiO1 (mag)	0.029 ± 0.001	-0.032 ± 0.002
TiO2 (mag)	0.045 ± 0.001	-0.026 ± 0.002
B4000	-0.128 ± 0.003	0.848 ± 0.006
HK	-0.064 ± 0.003	1.003 ± 0.008
HδF	-1.600 ± 0.044	4.032 ± 0.099
HγF	-2.530 ± 0.046	4.333 ± 0.104

3.2 Index values as a function of radius

The spatial gradients we measure here describe the *mean index value in apertures of varying radii*, at fixed σ. This is in contrast with 'true' spatial index gradients, which are measured in increasing annuli projected on the galaxy. As a result, the values we measure are smaller in magnitude than the true gradients. Our values, which we give in Table 1, are, however, directly applicable to aperture correction.

All the narrow-line indices, with the exception of HK, show a radial gradient. The gradients are negative except for the hydrogen line indices and the 4000 Å break, B4000. Additionally, some indices show a well-defined trend of index gradient with σ (these can be quickly identified in the last column of Table 1). In all the cases (except CN1 and CN2), the sense of this variation is that the index gradient becomes less steep with increasing σ. In some cases, including Hβ, a significant index gradient at low values of σ disappears completely for $\sigma > 250\,\mathrm{km\,s^{-1}}$. We find no dependence on the radial index gradients with density of environment at fixed σ. The fact that some indices show gradients which decrease with increasing σ does not necessarily imply that some process has acted to mix the stellar populations in more massive systems. We return to this below.

3.3 Stellar population trends

We now make use of a subset of the index values to derive the age, metallicity and α-enhancement of the galaxy population in

our sample. We repeat the multiple linear regression procedure described in Paper I, using the same indices (but excluding G4300). We briefly summarize the procedure here.

First, because our index values are not calibrated to the Lick system (due to the lack of Lick standard star spectra in SDSS), we consider index variations relative to the mean value at a σ of $\sigma = 200\,\mathrm{km\,s^{-1}}$. By working with these differential index values, we avoid both the problem of absolute calibration to the Lick system and potential problems in the absolute calibration of the SSP models. We therefore perform a multiple linear regression according to equation (5) of Paper I. The linear regression is performed on the whole sample and on two subsets of environmental density, $1/r_5 \leq 0.5$ (typical of the 'field') and $1/r_5 \geq 1.5$ (more typical of a cluster). We also perform the analysis on indices aperture corrected to two different radii, $r_e/2$ and $r_e/4$, to investigate radial trends within the individual galaxies.

The results of this regression analysis showed that the carbon abundance did not depend on σ, having a constant offset as a function of environment, in contrast to Paper I. This difference is probably due to the better aperture correction used here and/or the exclusion of the G4300 index. We therefore remove the explicit carbon abundance from the regression analysis, allowing the carbon abundance to be included in the metallicity term. The *simultaneous a posteriori fit* of the model to three example indices is compared with the median of the data in the different bins of σ, in Fig. 1.

In the left-hand panel of Fig. 2, we show the results for the entire sample for two different radii. For $r_e/4$, the trend of age with σ is very similar to that seen in Paper I with a steady rise in age from the lowest mass systems and an approximately constant age for galaxies with $\sigma > 230\,\mathrm{km\,s^{-1}}$. For the larger aperture, however, the trend is slightly different, with a less pronounced flattening towards high values of σ. For $\sigma > 300\,\mathrm{km\,s^{-1}}$, the mean age is $\simeq$0.05 dex older for $r_e/2$ compared to $r_e/4$. This corresponds to an age difference of $\sim$1 Gyr for a galaxy of age 10 Gyr. The crossover point of the two lines in the top panel of Fig. 2 shows that galaxies with $\sigma > 180\,\mathrm{km\,s^{-1}}$ have positive radial age gradients. Neither Sánchez-Blázquez et al. (2007) nor Mehlert et al. (2003) find evidence of radial age gradients in ETGs. We derive an age gradient in massive galaxies *despite the absence of a gradient of the Hβ index*.

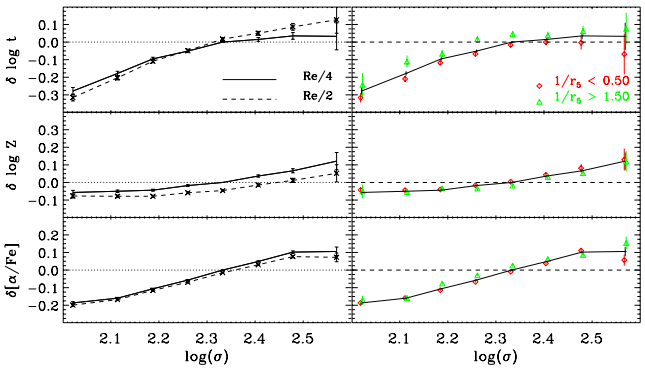

Figure 2. Age, metallicity and α-enhancement variations as a function of σ. A linear regression analysis has been carried out simultaneously on the Hβ, Hδ, Mg1, Mg2, Mgb, Fe4383, Fe4531, Fe5270, Fe5335 and C4668 indices. Left-hand panel: radial variation. The two lines in each plot refer to index values corrected to $r_e/4$ (solid line) and $r_e/2$ (dashed line). Right-hand panel: effect of environment. The solid line represents the entire sample, diamonds only those objects in low-density environments ($1/r_5 < 0.5$) and triangles only those in high-density environments ($1/r_5 > 1.5$). Values are differences with respect to those of the entire sample at $\sigma = 200\,\mathrm{km\,s^{-1}}$. The central σ bins typically contain $>10^3$ galaxies, whereas the highest bin contains only 16.

The increase in metallicity with σ is less strong than that found in Paper I. The gradient for the indices, corrected to $r_e/4$, for $\sigma > 160\,\mathrm{km\,s^{-1}}$ is d log (Z)/d log $(\sigma) \simeq 0.42$. This value is similar to that found by N05, Thomas et al. (2005) and Smith et al. (2007) but smaller than that of Kuntschner et al. (2001). For $\sigma < 160\,\mathrm{km\,s^{-1}}$, however, there is no significant trend of index value with σ. For the $r_e/2$ aperture, the metallicity is $\simeq$0.05 dex lower so that ETGs are less metal rich at larger radii. Negative metallicity gradients have also been reported by Proctor et al. (2008), Annibali et al. (2007), Sánchez-Blázquez et al. (2007) and Harris & Harris (2002). There is also evidence that the metallicity gradients are steeper for more massive galaxies as found by Forbes, Sánchez-Blázquez & Proctor (2005). The metallicity gradient likely compensates the age gradient to remove radial gradients in indices like Hβ.

The trend of α-enhancement with σ is also slightly less steep than found in Paper I, with d$[\alpha/\mathrm{Fe}]$/d log$(\sigma) \simeq 0.55$, similar to that found by Annibali et al. (2007) but steeper than the $\sim$0.3 found by several authors (Kuntschner et al. 2001, N05; Thomas et al. 2005; Bernardi et al. 2006; Smith et al. 2007). Although most similar studies refer to a smaller radius, we see that the larger aperture, $r_e/2$, has a marginally shallower gradient. The α-enhancement within this larger aperture is slightly lower, with the difference being largest (0.03 dex) for the most massive galaxies. This does not support the 'outside-in' ETG formation scenario (Pipino, Matteucci & Chiappini 2006). A negative α-enhancement gradient is also seen in the halo stars of the Galaxy (Fulbright 2000).

In the right-hand panel of Fig. 2, we show the variation of evolutionary parameters as a function of the density of environment for index values aperture corrected to $r_e/4$. In both the environments, the increase in age with σ is similar, with a flattening above $\sigma \sim 200\,\mathrm{km\,s^{-1}}$. Objects in dense environments ($1/r_5 \geq 1.5$), however, are 0.087 dex older than those in less dense environments ($1/r_5 \leq 0.5$). This is a difference of 2 Gyr if the ages are close to 10 Gyr and is consistent with several earlier studies (Kuntschner et al. 2002; Terlevich & Forbes 2002; Sánchez-Blázquez et al. 2006; de la Rosa et al. 2007). The flattening of the age–σ relation is also slightly more pronounced for the lower density environment. Similar age trends were seen in Paper I.

There is marginal evidence that the metallicity is lower in high-density environments. Formally, the difference is 0.020 ± 0.013 dex. Thomas et al. (2005) also found a small environmental dependence on the metallicity in the same sense and de la Rosa et al. (2007) find a difference of 0.11 dex between Hickson Compact Groups and the field. Other authors have found both larger differences in the same sense (Kuntschner et al. 2002; Proctor et al. 2004), no effect (Bernardi et al. 2006; Annibali et al. 2007) and the opposite effect (Gallazzi et al. 2006; Mateus et al. 2007). In Paper I, no difference was found.

No environmental effect is found for the α-enhancement, in agreement with Kuntschner et al. (2002), Thomas et al. (2005), Annibali et al. (2007) and Gallazzi et al. (2006). However, Proctor et al. (2004), Bernardi et al. (2006) and Lucey et al. (2007) all find increased α-enhancement in denser environments.

4 DISCUSSION AND CONCLUSIONS

We find positive correlations between age, metallicity and α-enhancement and the velocity dispersion, σ, in ETGs. Galaxies in dense environments are $\sim$20 per cent older than those in

low-density environments for all σ ($\sim$2 Gyr for an age of 10 Gyr). The trend with age flattens above $\sigma \sim 200\,\mathrm{km\,s^{-1}}$, especially for galaxies in low-density environments. We find a marginally significant trend towards higher metallicities in low-density environments but the environment has no effect on the α-enhancement.

Apart from the marginal metallicity difference between field and cluster, the results are very similar to those of Paper I. There we concluded that an antihierarchical scenario, in which star formation lasts longer but with lower efficiency in lower mass objects (see Granato et al. 2004), was consistent with the data. Here, the additional determination of SSP parameters as a function of galactic radius places additional constraints on the evolutionary scenario.

Massive ETGs ($\sigma > 180\,\mathrm{km\,s^{-1}}$) have positive radial age gradients, negative metallicity gradients and marginally significant negative α-enhancement gradients. When a massive halo becomes nonlinear, it accretes smaller haloes which started to collapse at earlier times. The radial trends suggest that these haloes do not contain only gas, but also pristine stars. The gaseous component falls dissipatively into the potential well of the massive (proto)spheroid, fuelling rapid star formation. The increase in mass increases the rate and efficiency of star formation, driving the main correlations with galaxy mass. The pristine stellar component of each subhalo, however, being dissipationless, is deposited at a radius consistent with the angular momentum of the encounter. These stars, which are slightly older, more metal poor and have moderate α-enhancement will therefore be spread over larger radii. At early times, rapid gas-rich mergers lead to an almost monolithic formation, at later times mergers become increasingly 'dry'. Very similar scenarios have been proposed to explain both the bimodal metallicity distribution of globular clusters and the greater radial scalelength of metal-poor relative to metal-rich globular clusters in elliptical galaxies (Côté, Marzke & West 1998; Bekki et al. 2008). Our results imply that the metal-poor globular cluster population in ETGs should be older, less metal rich and slightly less α-enhanced than the metal-rich clusters.

Because the age difference at larger radii is actually the luminosity-weighted SSP equivalent age in a larger aperture (not an annulus), the value of 0.05 dex, $\sim$1 Gyr, is a lower limit to the real age difference at larger radii. This time difference limits the assembly redshift of massive ETGs simply due to the lack of time to accommodate the formation of stars in the lower mass haloes. Our limit translates into an upper limit to the assembly redshift of massive ETGs of $z \lesssim 3.5$; in which case the stars in low-mass haloes formed at $z \sim 10$, for a standard cosmology ($H_0 = 70$, $\Omega_\mathrm{m} = 0.3$, $\Omega_\Lambda = 0.7$). This also provides an estimate of the star formation rate in the assembled spheroid. If the final stellar mass were $10^{12}\,\mathrm{M_\odot}$ then stars must have formed at a rate $\sim 10^{12}\,\mathrm{M_\odot}/1\,\mathrm{Gyr} \sim 10^3\,\mathrm{M_\odot\,yr^{-1}}$.

We conclude by stressing the statistical nature of our results. Because a galaxy's velocity dispersion is a function of both the halo mass and virialization redshift, variations in these parameters may render small samples insensitive to the trends we find.

The catalogue on which this article is based can be found at www.mrao.cam.ac.uk/$\sim$bn204/galevol/clemensetal08.html.

ACKNOWLEDGMENTS

Funding for the SDSS and SDSS-II has been provided by the Alfred P. Sloan Foundation, the Participating Institutions, the National Science Foundation, the US Department of Energy, the National Aeronautics and Space Administration, the Japanese Monbukagakusho, the Max Planck Society and the Higher Education Funding Council for England. The SDSS web site is http://www.sdss.org/. We acknowledge a financial contribution from contract ASI-INAF I/016/07/0.

REFERENCES

Adelman-McCarthy J. K. et al., 2007, ApJS, 172, 634
Annibali F., Bressan A., Rampazzo R., Zeilinger W. W., Danese L., 2007, A&A, 463, 455
Bekki K., Yahagi H., Nagashima M., Forbes D. A., 2008, MNRAS, 387, 1131
Bernardi M. et al., 2003, AJ, 125, 1882 (B03)
Bernardi M., Nichol R. C., Sheth R. K., Miller C. J., Brinkmann J., 2006, AJ, 131, 1288
Bressan A. et al., 2006, ApJ, 639, L55
Clemens M. S., Bressan A., Nikolic B., Alexander P., Annibali F., Rampazzo R., 2006, MNRAS, 370, 702 (Paper I)
Clemens M. S., Bressan A., Panuzzo P., Rampazzo R., Silva L., Buson L., Granato G. L., 2008, MNRAS, in press (arXiv:0808.2899)
Côté P., Marzke R. O., West M. J., 1998, ApJ, 501, 554
de la Rosa I. G., de Carvalho R. R., Vazdekis A., Barbuy B., 2007, AJ, 133, 330
Forbes D. A., Sánchez-Blázquez P., Proctor R., 2005, MNRAS, 361, L6
Fulbright J. P., 2000, AJ, 120, 1841
Gallazzi A., Charlot S., Brinchmann J., White S. D. M., 2006, MNRAS, 370, 1106
Granato G. L., De Zotti G., Silva L., Bressan A., Danese L., 2004, ApJ, 600, 580
Harris W. E., Harris G. L. H., 2002, AJ, 123, 3108
Jimenez R., Bernardi M., Haiman Z., Panter B., Heavens A. F., 2007, ApJ, 669, 947
Kuntschner H., Lucey J. R., Smith R. J., Hudson M. J., Davies R. L., 2001, MNRAS, 323, 615
Kuntschner H., Smith R. J., Colless M., Davies R. L., Kaldare R., Vazdekis A., 2002, MNRAS, 337, 172
Lucey J. R., Smith R. J., Hudson M. J., Nelan J. E., Wegner G. A., 2007, in Metcalfe N., Shanks T., eds, ASP Conf. Ser. Vol. 379 Cosmic Frontiers. Astron. Soc. Pac., San Francisco, p. 117
Mateus A., Sodré L., Cid Fernandes R., Stasińska G., 2007, MNRAS, 374, 1457
Mehlert D., Thomas D., Saglia R. P., Bender R., Wegner G., 2003, A&A, 407, 423
Nelan J. E., Smith R. J., Hudson M. J., Wegner G. A., Lucey J. R., Moore S. A. W., Quinney S. J., Suntzeff N. B., 2005, ApJ, 632, 137 (N05)
Pipino A., Matteucci F., Chiappini C., 2006, ApJ, 638, 739
Proctor R. N., Forbes D. A., Hau G. K. T., Beasley M. A., De Silva G. M., Contreras R., Terlevich A. I., 2004, MNRAS, 349, 1381
Proctor R. N., Lah P., Forbes D. A., Colless M., Couch W., 2008, MNRAS, 386, 1781
Rampazzo R., Annibali F., Bressan A., Longhetti M., Padoan F., Zeilinger W. W., 2005, A&A, 433, 479
Rogers B., Ferreras I., Lahav O., Bernardi M., Kaviraj S., Yi S. K., 2007, MNRAS, 382, 750
Sánchez-Blázquez P., Gorgas J., Cardiel N., González J. J., 2006, A&A, 457, 809
Sánchez-Blázquez P., Forbes D. A., Strader J., Brodie J., Proctor R., 2007, MNRAS, 377, 759
Schawinski K. et al., 2007, ApJS, 173, 512
Smith R. J., Lucey J. R., Hudson M. J., 2007, MNRAS, 381, 1035
Terlevich A. I., Forbes D. A., 2002, MNRAS, 330, 547
Thomas D., Maraston C., Bender R., Mendes de Oliveira C., 2005, ApJ, 621, 673

This paper has been typeset from a TEX/LATEX file prepared by the author.